UDC 551.509.313

An Implicit Time Integration Scheme for Baroclinic Models of the Atmosphere

ANDRÉ ROBERT, JOHN HENDERSON, and COLIN TURNBULL—*Meteorological Service of Canada, Montreal, Quebec, Canada*

ABSTRACT—A semi-implicit time integration algorithm developed earlier for a barotropic model resulted in an appreciable economy of computing time. An extension of this method to baroclinic models is formulated, including a description of the various steps in the calculations. In the proposed scheme, the temperature is separated into a basic part dependent only on the vertical coordinate and a corresponding perturbation part. All terms involving the perturbation temperature are calculated from current values of the variables, while a centered finite-difference time average is applied to the horizontal pressure gradient, the divergence, and the vertical motion in the remaining terms. This method gives computationally stable integrations with relatively large time steps.

The model used to test the semi-implicit scheme does not include topography, precipitation, diabatic heating, and other important physical processes. Five-day hemispheric integrations from real data with time steps of 60 and 30 min show differences of the order of 3 m. These errors are insignificant when compared to other sources of error normally present in most numerical models. Presently, this model produces relatively good short-range predictions, and this is a strong factor in favor of inserting the major physical processes as soon as possible.

1. INTRODUCTION

Modelers use a wide variety of numerical time integration schemes for their experiments. For instance, Smagorinsky et al. (1965) use centered differences, Kasahara and Washington (1967) apply a modified version of the Lax-Wendroff scheme, and Mintz (1965) uses the backward differencing scheme of Matsuno. This seems surprising when one considers that the various time integration algorithms differ so much from each other that a simple investigation should reveal which one of these will provide the best performance. In fact, some authors have performed comparisons involving many frequently used schemes. As examples, we find an investigation of 13 different computational methods performed by Young (1968). Also, Lilly (1965) and Kurihara (1965) studied the properties of a number of time integration techniques. The accumulation of analytic and experimental evidence did not succeed in reducing the number of integration algorithms considered by atmospheric scientists.

The following sections of this paper will not alleviate the problem since they introduce and describe a semi-implicit method of integration, thereby adding another element to an already voluminous assortment of techniques. Fortunately, this method has a significant advantage. It operates with a time step of 60 min in a model where a short 10-min time step is normally required. The truncation errors associated with the large time step appear to be insignificantly small so that there is no penalization for the substantial increase in computational efficiency.

Until recently, very little attention has been paid, to the implicit and semi-implicit methods, by the atmospheric scientists outside the U.S.S.R. Thompson (1961) devotes only a few lines to this subject. In the U.S.S.R., Marchuk (1965) investigated this field extensively and developed a number of highly efficient and practical algorithms. Subsequently, Kurihara (1965) and Holton (1967) applied the implicit method to linear equations. Nonlinear barotropic integrations were performed later with a spectral model by Robert (1969) and with gridpoint models by Kwizak and Robert (1971) and McPherson (1971). The purpose of this paper is to report on experiments performed with a semi-implicit time integration algorithm in a baroclinic model that will soon be used in Canada for short-range weather forecasting.

2. THE MODELING EQUATIONS

In principle, the model described by Shuman and Hovermale (1968) was adopted for the experiments with the semi-implicit algorithm. This is the model currently used at the National Meteorological Center (NMC), Suitland, Md., for the production of weather forecasts on a routine basis. As suggested later by Shuman and Stackpole (1969), the original formulation was changed slightly to use the invariant form of the meteorological equations.

In the experiments with the barotropic version, Kwizak and Robert (1971) used the same space differences as in the NMC model. A few slight modifications, introduced to reduce truncation errors in the additional

operations required in the integration scheme, are described by the authors in their paper.

Noticeable changes were made in the formulation and in the finite differences related to the vertical coordinate in the baroclinic version. A derivation of the model will be given to describe these modifications. We will use the hydrostatic approximation and introduce a vertical coordinate σ as follows:

$$\frac{\sigma}{\sigma_s}=\frac{p}{p_s} \tag{1}$$

where the subscript, s, represents values at the lower boundary, and σ_s is a constant used for scaling σ. The equations will then take the form

$$\frac{du}{dt}-v\left(f+\frac{u}{a}\tan\varphi\right)=-\frac{\partial\phi}{\partial x}-\frac{RT}{p_s}\frac{\partial p_s}{\partial x}+F_x, \tag{2}$$

$$\frac{dv}{dt}+u\left(f+\frac{u}{a}\tan\varphi\right)=-\frac{\partial\phi}{\partial y}-\frac{RT}{p_s}\frac{\partial p_s}{\partial y}+F_y, \tag{3}$$

$$c_p\frac{dT}{dt}=RT\left(\frac{\dot\sigma}{\sigma}+\frac{1}{p_s}\frac{dp_s}{dt}\right)+H, \tag{4}$$

$$\frac{\partial p_s}{\partial t}=-\nabla\cdot(p_s\tilde{\mathbf{V}}), \tag{5}$$

$$p_s\frac{\partial\dot\sigma}{\partial\sigma}=-\nabla\cdot p_s(\mathbf{V}-\tilde{\mathbf{V}}), \tag{6}$$

and

$$\frac{\partial\phi}{\partial\sigma}+\frac{RT}{\sigma}=0 \tag{7}$$

where the symbol (~) represents the vertical average

$$\tilde{\mathbf{V}}=\frac{1}{\sigma_s}\int_0^{\sigma_s}\mathbf{V}\partial\sigma \tag{8}$$

and

$$\nabla=\boldsymbol{i}\frac{\partial}{\partial x}+\boldsymbol{j}\frac{\partial}{\partial y}. \tag{9}$$

The equations given above are valid in spherical polar coordinates where x represents the distance measured eastward along latitude circles and y represents the distance measured northward along meridians. The variables u, v, and $\dot\sigma$ are the components of the velocity vector in the curvilinear coordinates x, y, and σ. Some small terms involving the vertical component of the wind were neglected in the equation of motion and in the equation of continuity. The geopotential, the pressure, and the temperature are represented by ϕ, p, and T, respectively. Also, f is the Coriolis parameter, a is the radius of the earth, φ is the latitude, R is the gas constant for dry air, c_p is the heat capacity at constant pressure, H is the diabatic heating rate, and F_x and F_y represent the viscous dissipation terms.

The variables are defined at the points of a rectangular grid in a conformal projection. Also, a set of dimensionless variables will be introduced into the modeling equations for the numerical integrations. The only virtue of the dimensionless system resides in the fact that it simplifies the presentation of the semi-implicit treatment of the equations. This is the reason why it is used here. Now

$$\partial X=\frac{m}{d}\partial x \tag{10}$$

and

$$\partial Y=\frac{m}{d}\partial y. \tag{11}$$

In these equations, m represents the map scale factor, and d is the length used for scaling. The constants $\Delta\sigma$ and Δt will also be used for the same purpose, giving

$$Z=\frac{\sigma}{\Delta\sigma}, \tag{12}$$

$$\tau=\frac{t}{\Delta t}, \tag{13}$$

$$U=\frac{u\Delta t}{md}, \tag{14}$$

$$V=\frac{v\Delta t}{md}, \tag{15}$$

$$w=\frac{\dot\sigma\Delta t}{\Delta\sigma}, \tag{16}$$

$$\Phi=\frac{\phi\Delta t^2}{d^2}, \tag{17}$$

$$\theta=\frac{RT\Delta t^2}{d^2}, \tag{18}$$

$$\kappa=\frac{R}{c_p}, \tag{19}$$

$$F_X=\frac{F_x\Delta t^2}{md}, \tag{20}$$

$$F_Y=\frac{F_y\Delta t^2}{md}, \tag{21}$$

$$h=\frac{\kappa H\Delta t^3}{d^2}, \tag{22}$$

$$K=\frac{1}{2}m^2(U^2+V^2), \tag{23}$$

$$Q=f\Delta t+m^2\left(\frac{\partial V}{\partial X}-\frac{\partial U}{\partial Y}\right), \tag{24}$$

and

$$A=\frac{m^2}{p_s}\left(U\frac{\partial p_s}{\partial X}+V\frac{\partial p_s}{\partial Y}\right). \tag{25}$$

After these substitutions are made, the original equations will take the following form:

$$\frac{\partial U}{\partial\tau}-QV+\frac{\partial K}{\partial X}+w\frac{\partial U}{\partial Z}=-\frac{\partial\Phi}{\partial X}-\frac{\theta}{p_s}\frac{\partial p_s}{\partial X}+F_X, \tag{26}$$

$$\frac{\partial V}{\partial\tau}+QU+\frac{\partial K}{\partial Y}+w\frac{\partial V}{\partial Z}=-\frac{\partial\Phi}{\partial Y}-\frac{\theta}{p_s}\frac{\partial p_s}{\partial Y}+F_Y, \tag{27}$$

$$\frac{d\theta}{d\tau}=h+\kappa\theta\left[\frac{w}{Z}-m^2\left(\frac{\partial\tilde U}{\partial X}+\frac{\partial\tilde V}{\partial Y}\right)+A-\tilde A\right], \tag{28}$$

$$\frac{\partial p_s}{\partial \tau}=-m^2 p_s\left(\frac{\partial \tilde{U}}{\partial X}+\frac{\partial \tilde{V}}{\partial Y}\right)-p_s\tilde{A}, \tag{29}$$

$$\frac{\partial w}{\partial Z}=-m^2\left[\frac{\partial}{\partial X}(U-\tilde{U})+\frac{\partial}{\partial Y}(V-\tilde{V})\right]-(A-\tilde{A}), \tag{30}$$

and

$$\frac{\partial \Phi}{\partial Z}=-\frac{\theta}{Z}. \tag{31}$$

Note that the map scale factor appears in the modified horizontal wind components defined in eq (14) and (15). Also, eq (26) and (27) appear in their invariant form. With these changes, there is no explicit reference to terms containing derivatives of the map scale factor.

Equations (26)–(31) are valid in any Cartesian system, so there is an advantage in using the coordinates defined by the grid. This will be done in the numerical integrations, and in the calculations, U and V will represent the components of the horizontal wind vector along the axes of the grid network.

3. MODIFICATIONS FOR THE IMPLICIT SCHEME

A variable, θ^*, dependent only on the vertical coordinate and the two following variables,

$$P=\Phi+\theta^*\ln p_s \tag{32}$$

and

$$W=w-Zm^2\left(\frac{\partial \tilde{U}}{\partial X}+\frac{\partial \tilde{V}}{\partial Y}\right)-Z\tilde{A} \tag{33}$$

will be used in the calculations.

The static stability and some additional terms appearing in the meteorological equations will be defined as follows:

$$\gamma=\frac{1}{Z}\left(\frac{\kappa\theta}{Z}-\frac{\partial\theta}{\partial Z}\right), \tag{34}$$

$$B=m^2\left(U\frac{\partial^2 P}{\partial X\partial Z}+V\frac{\partial^2 P}{\partial Y\partial Z}\right), \tag{35}$$

$$\gamma^*=\frac{1}{Z}\left(\frac{\kappa\theta^*}{Z}-\frac{\partial\theta^*}{\partial Z}\right), \tag{36}$$

$$\theta'=\theta-\theta^*, \tag{37}$$

$$\gamma'=\gamma-\gamma^*, \tag{38}$$

and

$$\epsilon=\frac{\theta_s^*}{Z_s}. \tag{39}$$

The variable θ taken from the hydrostatic approximation [eq (31)] is substituted into the time derivative and the horizontal advection term of the thermodynamic equation [eq (28)]. Then the geopotential, Φ, taken from eq (32) is substituted into eq (26) and (27) and where it appears explicitly in eq (28). Also, the variable w taken from eq (33) is substituted in eq (28) and (30). Finally, by applying eq (32) at the lower boundary, we may express p_s in terms of P_s and Φ_s and substitute in eq (29). These modifications are tedious but do not involve any serious difficulties. The resulting equations appear as follows:

$$\frac{\partial U}{\partial \tau}+\frac{\partial P}{\partial X}=r_1, \tag{40}$$

$$r_1=QV-\frac{\partial K}{\partial X}-w\frac{\partial U}{\partial Z}-\frac{\theta'}{p_s}\frac{\partial p_s}{\partial X}+F_X, \tag{41}$$

$$\frac{\partial V}{\partial \tau}+\frac{\partial P}{\partial Y}=r_2, \tag{42}$$

$$r_2=-QU-\frac{\partial K}{\partial Y}-w\frac{\partial V}{\partial Z}-\frac{\theta'}{p_s}\frac{\partial p_s}{\partial Y}+F_Y, \tag{43}$$

$$\frac{\partial^2 P}{\partial \tau\partial Z}+\gamma^* W=r_3, \tag{44}$$

$$r_3=-\frac{h}{Z}-B-\gamma' W-\frac{W_s}{Z_s}\frac{\partial\theta'}{\partial Z}+A\left(\frac{\partial\theta^*}{\partial Z}-\frac{\kappa\theta}{Z}\right), \tag{45}$$

$$\frac{\partial P_s}{\partial \tau}-\epsilon W_s=0, \tag{46}$$

and

$$\frac{\partial W}{\partial Z}+m^2\left(\frac{\partial U}{\partial X}+\frac{\partial V}{\partial Y}\right)=-A. \tag{47}$$

It is important to note that the above transformations were made without any approximations. The quantities r_1, r_2, and r_3 will be evaluated first, and the implicit method will be applied to the remaining calculations.

4. THE SEMI-IMPLICIT ALGORITHM

The following finite-difference approximations will be used for the time integration:

$$F_\tau=\frac{F(\tau+1)-F(\tau-1)}{2} \tag{48}$$

and

$$\overline{F}^\tau=\frac{F(\tau+1)+F(\tau-1)}{2}, \tag{49}$$

and these operators will be applied as follows:

$$U_\tau+\frac{\overline{\partial P}^\tau}{\partial X}=r_1, \tag{50}$$

$$V_\tau+\frac{\overline{\partial P}^\tau}{\partial Y}=r_2, \tag{51}$$

$$\left(\frac{\partial P}{\partial Z}\right)_\tau+\gamma^*\overline{W}^\tau=r_3, \tag{52}$$

$$(P_s)_\tau-\epsilon\overline{W}_s^\tau=0, \tag{53}$$

and

$$\frac{\overline{\partial W}^\tau}{\partial Z}+m^2\left(\frac{\overline{\partial U}^\tau}{\partial X}+\frac{\overline{\partial V}^\tau}{\partial Y}\right)=-A. \tag{54}$$

These equations may now be transformed into the following:

$$\overline{U}^\tau+\frac{\overline{\partial P}^\tau}{\partial X}=q_1, \tag{55}$$

$$\overline{V}^{\tau}+\frac{\overline{\partial P}^{\tau}}{\partial Y}=q_2, \tag{56}$$

$$\frac{\overline{\partial P}^{\tau}}{\partial Z}+\gamma^*\overline{W}^{\tau}=-C, \tag{57}$$

and

$$\overline{P}_s^{\tau}-\epsilon\overline{W}_s^{\tau}=C_s \tag{58}$$

where

$$q_1=U(\tau-1)+r_1, \tag{59}$$

$$q_2=V(\tau-1)+r_2, \tag{60}$$

$$C=-\frac{\partial P}{\partial Z}(\tau-1)-r_3, \tag{61}$$

and

$$C_s=P_s(\tau-1). \tag{62}$$

We will now use eq (55) and (56) to eliminate the divergence from eq (54) giving

$$\frac{\overline{\partial W}^{\tau}}{\partial Z}-m^2\nabla^2\overline{P}^{\tau}=m^2D \tag{63}$$

where

$$D=-\frac{A}{m^2}-\left(\frac{\partial q_1}{\partial X}+\frac{\partial q_2}{\partial Y}\right). \tag{64}$$

The integration procedure will consist of evaluating A, B, r_1, r_2, r_3, and then q_1, q_2, C, and D. At this point, we still have to solve eq (57), (58), and (63) for the two unknown variables contained in these equations.

5. THE VERTICAL REPRESENTATION

In the current version of the model, it is possible to perform integrations with as many as seven levels and the allowable maximum number of levels will soon be increased to 15. All the tests reported in the following sections were performed with five levels. To keep the description of the vertical representation as short as possible, we will consider a three-level version as shown in figure 1. The generalization to an arbitrary number of levels will not present any difficulties.

As we can see from figure 1, the variables P and W are staggered with respect to each other. If we apply eq (57), (58), and (63) to their respective levels, we get the following set of equations:

$$\nabla^2\overline{P}_1^{\tau}-\frac{1}{m^2}\overline{W}_2^{\tau}=-D_1, \tag{65}$$

$$\overline{P}_1^{\tau}-\overline{P}_3^{\tau}-\frac{\lambda_2}{m^2}\overline{W}_2^{\tau}=C_2, \tag{66}$$

$$\nabla^2\overline{P}_3^{\tau}+\frac{1}{m^2}(\overline{W}_2^{\tau}-\overline{W}_4^{\tau})=-D_3, \tag{67}$$

$$\overline{P}_3^{\tau}-\overline{P}_5^{\tau}-\frac{\lambda_4}{m^2}\overline{W}_4^{\tau}=C_4, \tag{68}$$

$$\nabla^2\overline{P}_5^{\tau}+\frac{1}{m^2}(\overline{W}_4^{\tau}-\overline{W}_6^{\tau})=-D_5, \tag{69}$$

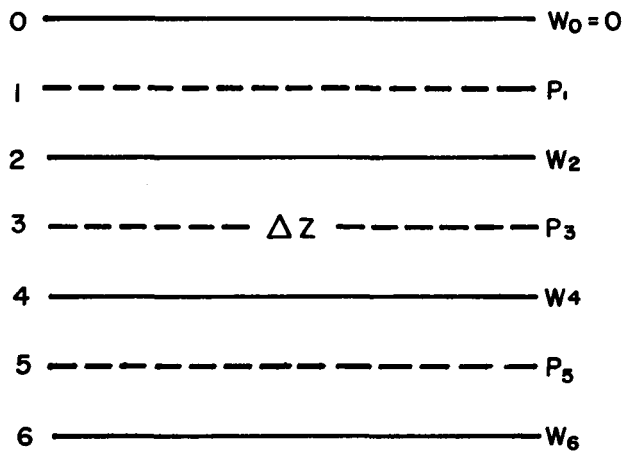

FIGURE 1.—The distribution of levels in the model. The wind and the geopotential are given at the odd levels. Temperature and vertical motion appear at the even levels.

and

$$\overline{P}_s^{\tau}-\frac{\lambda_5}{m^2}\overline{W}_s^{\tau}=C_s. \tag{70}$$

In the above equations, the subscripts represent the level at which the variable is taken as indicated in figure 1, and level six represents the lower boundary also represented by the subscript s. Also,

$$\lambda=m^2\gamma^* \tag{71}$$

and

$$\lambda_s=m^2\epsilon. \tag{72}$$

If we eliminate the variable W from the above set of equations, we get

$$\nabla^2\overline{P}_1^{\tau}-\left(\frac{\overline{P}_1^{\tau}-\overline{P}_3^{\tau}}{\lambda_2}\right)=G_1, \tag{73}$$

$$\nabla^2\overline{P}_3^{\tau}-\left(\frac{\overline{P}_3^{\tau}-\overline{P}_5^{\tau}}{\lambda_4}\right)+\left(\frac{\overline{P}_1^{\tau}-\overline{P}_3^{\tau}}{\lambda_2}\right)=G_3, \tag{74}$$

and

$$\nabla^2\overline{P}_5^{\tau}-\frac{\overline{P}_s^{\tau}}{\lambda_s}+\left(\frac{\overline{P}_3^{\tau}-\overline{P}_5^{\tau}}{\lambda_4}\right)=G_5, \tag{75}$$

where

$$G_1=D_1-\frac{C_2}{\lambda_2}, \tag{76}$$

$$G_3=-D_3-\frac{C_4}{\lambda_4}+\frac{C_2}{\lambda_2}, \tag{77}$$

and

$$G_5=-D_5-\frac{C_s}{\lambda_s}+\frac{C_4}{\lambda_4}. \tag{78}$$

We find that eq(73)–(75) may be written as a single differential equation in three dimensions; that is,

$$\nabla^2\overline{P}^{\tau}+\frac{\partial}{\partial Z}\left(\frac{1}{\lambda}\frac{\partial\overline{P}^{\tau}}{\partial Z}\right)=G, \tag{79}$$

and, given G, we must solve for $\overline{P}^{\tau}$ with the boundary con-

ditions

$$\frac{\partial \overline{P}^{\tau}}{\partial Z}=0 \tag{80}$$

at the top boundary and

$$\frac{\partial \overline{P}^{\tau}}{\partial Z}=-\frac{\overline{P}^{\tau}}{\lambda} \tag{81}$$

at the lower boundary. At the lateral boundaries, we will use the condition used by Shuman and Hovermale (1968) that the gradient of the geopotential normal to the boundary is in geostrophic equilibrium with the tangential flow. In terms of the variable P, this condition appears as

$$\frac{\partial \overline{P}^{\tau}}{\partial n}=(f\Delta t)V_T-\frac{\theta'}{p_s}\frac{\partial p_s}{\partial n} \tag{82}$$

where ∂n is normal to the boundary measured positive outward, and V_T is the tangential flow measured counterclockwise around the grid.

The differential equation given in eq (79) is now in its general form and may be applied to as many levels as we wish, provided that we apply the given conditions at the boundaries. This is a second-order elliptic differential equation in three dimensions. It may be solved by Liebmann relaxation (Thompson 1961, p. 96) or any other iterative procedure. The coefficient of relaxation will depend on the number of levels used in the model and on the variable λ. An optimum coefficient of relaxation is obtained by evaluating the convergence rates for different values. This method seems adequate, and, in the five-level model used at present, a sufficiently accurate solution is obtained with 14 iterations.

Once that eq (79) has been solved for $\overline{P}^{\tau}$, the final steps of the forecast cycle proceed as follows:

$$\overline{U}^{\tau}=q_1-\frac{\partial \overline{P}^{\tau}}{\partial X}, \tag{83}$$

$$\overline{V}^{\tau}=q_2-\frac{\partial \overline{P}^{\tau}}{\partial Y}, \tag{84}$$

$$U(\tau+1)=2\overline{U}^{\tau}-U(\tau-1), \tag{85}$$

$$V(\tau+1)=2\overline{V}^{\tau}-V(\tau-1), \tag{86}$$

and

$$P(\tau+1)=2\overline{P}^{\tau}-P(\tau-1). \tag{87}$$

6. TIME INTEGRATIONS

The three preceding sections describe the formulation of the semi-implicit integration without giving any justification for this particular formulation. It is necessary at this point to add a few comments about the choice that was made. In each of eq (50)–(54), we could drop the terms appearing on the right-hand side. We would then have a system that would be valid for infinitesimally weak gravity waves in a stratified fluid at rest on a nonrotating sphere. Because this motion is given a fully implicit treatment, the time integration would then remain stable for time steps of any size.

If we treat explicitly the additional terms required when we wish to consider intense perturbations in a translating fluid on a rotating sphere, then there will be an upper limit to the size of the time step that can be used for the numerical integration. Linear analysis performed by Kwizak and Robert (1971) indicated that, for the conditions encountered in the atmosphere, the size of the time step would be restricted only by the short Rossby waves. Because this analysis does not apply to nonlinear equations and because it leaves some doubt even for linear equations, it seems advisable to test the scheme by performing some numerical integrations.

The constant pressure charts for 0000 GMT on Feb. 21, 1969, will be used for this experiment. Runs will be made with five σ-levels roughly equivalent to 100, 300, 500, 700, and 900 mb. The tests will be performed without any topography, surface friction, or other physical process. The model does not even include the vertical advection term in the wind equation, and a uniform value is used for the static stability at each level. These constraints are not intentional; they appear because these terms had not yet been incorporated in the model when the experiments were performed. Because the model is still incomplete, we must be careful in the interpretation of the results. The initialization will be carried out by the method suggested by Kwizak and Robert (1971). This scheme starts from analyses of the nondivergent part of the wind. The geopotential is generated from the nonlinear balance equation. The finite-difference approximations applied to the balance equation are identical to those used in the model. There is no divergence at initial time, and the initialization procedure does not allow any generation of divergence in the first time step. The rapid oscillations subsequently appearing during the time integrations have amplitudes of the order of a few meters.

A 5-day prediction of the 500-mb geopotential prepared with a 60-min time step is presented in figure 2. A similar prediction prepared with a 30-min step is also presented in figure 3. Visually, it is difficult to see the differences between the two predictions. To evaluate more objectively the dependence of the predictions on the size of the time step, we will evaluate the root-mean-square difference over the 51 $\times$ 55 grid every 6 hr for each level. The resulting curves are given in figure 4.

For the three lowest levels of the model, the curves differ by less than 0.3 m. They are so close to each other that it was not possible to include all of them in figure 4. For this reason, the curves for 700 and 900 mb are not shown in the figure. These errors grow to 3.5 m in 5 days. The rapid jump up to 2 m at the very beginning of the integration is probably due to the presence of weak gravity waves. Because of the weak vertical coupling in the model, the perturbations in the two upper levels move much too rapidly, and larger time truncation errors are associated with these translations.

462-836 O - 72 - 2

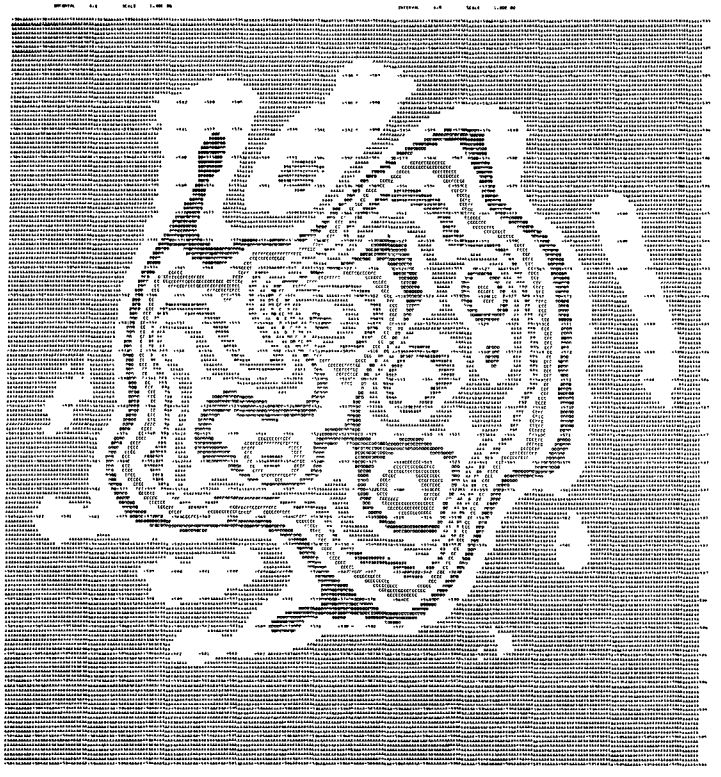

FIGURE 2.—Five-day prediction of the 500-mb geopotential prepared with a 60-min time step.

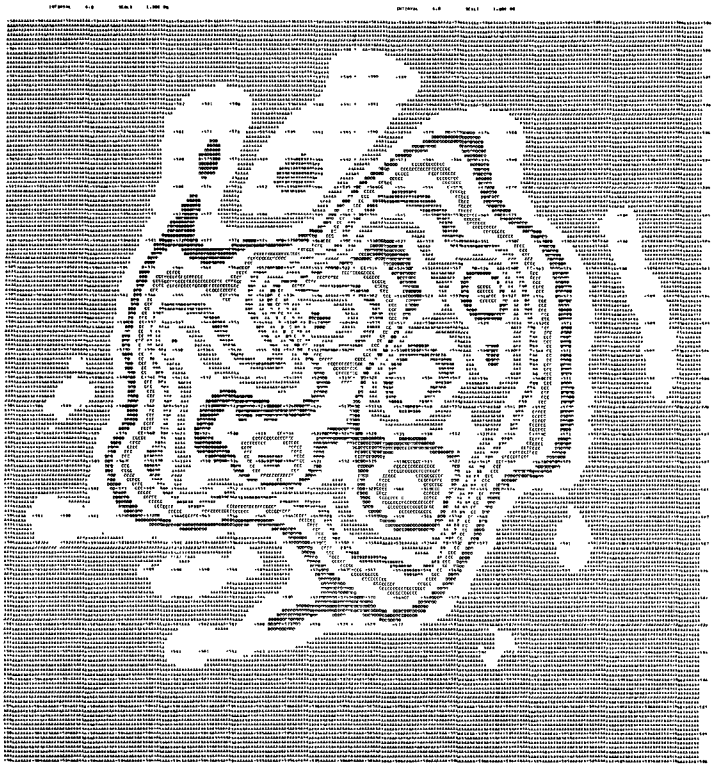

FIGURE 3.—Five-day prediction of the 500-mb geopotential prepared with a 30-min time step.

The truncation errors associated with the time differences are so small that there seems to be no point in determining their nature or searching for possible causes. At this stage, the semi-implicit leapfrog scheme clearly satisfies the accuracy requirements for short-range weather forecasting. We still need to test this algorithm in the presence of physical processes before we can draw a final conclusion. These experiments will be performed as soon as possible.

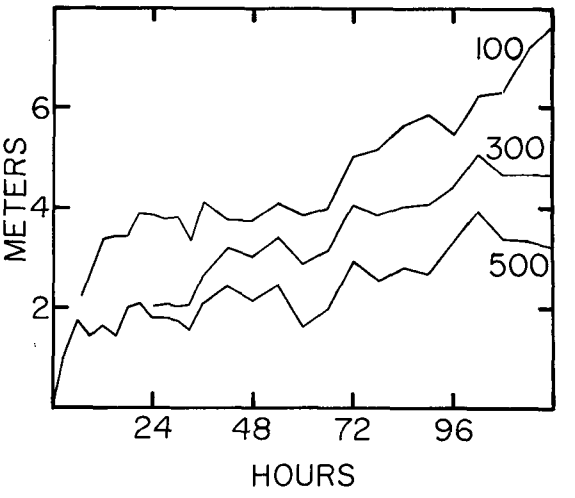

FIGURE 4.—Root-mean-square differences as a function of time between an integration with a 60-min time step and another integration with a 30-min step. The curves are for the 100-, 300-, and 500-mb levels.

TABLE 1.—*Root-mean-square error [RMSE (m)] and S1 scores for 36-hr predictions of the 500-mb geopotential over North America using the implicit and Canadian operational filtered models. All predictions were prepared from the 0000 GMT analyses, one for each of the first 8 mo of 1971. The dates were selected at random.*

Date	Implicit		Filtered	
	RMSE	S1	RMSE	S1
Jan. 14, 1971	112. 9	71	116. 7	68
Feb. 5, 1971	81. 0	47	71. 5	49
Mar. 26, 1971	86. 8	71	71. 6	72
Apr. 22, 1971	50. 7	55	52. 2	56
May 4, 1971	63. 7	59	67. 6	62
June 19, 1971	39. 0	56	36. 8	55
July 2, 1971	33. 0	52	26. 9	51
Aug. 21, 1971	48. 2	57	53. 1	61

The model has also been used to prepare some short-range forecasts. The integrations were performed with five levels and a time step of 1 hr. For these runs, the vertical advection terms and the variable static stability were available and were included in the integrations. A set of eight 36-hr forecasts was prepared and the verification scores are given in table 1. For comparison, the scores of the operational Canadian baroclinic model are also given. This is a four-level filtered model that includes topography, surface friction, internal viscosity, diabatic heating, and precipitation.

The root-mean-square error in the 500-mb geopotential is given for both models. The 500-mb S1 scores used by Shuman and Hovermale (1968) are also presented. The verification is performed over an area covering North America and a small portion of the adjacent oceans. For both schemes, a low value represents a good forecast. Even

without inclusion of any physical processes, we find that the semi-implicit model compares favorably with the filtered baroclinic model. These results are very encouraging since we can hope to get an additional improvement of the order of 7 m with the inclusion of the physical effects as they appear in the filtered model.

7. CONCLUSIONS

Experiments with a semi-implicit time integration algorithm applied to a baroclinic model of the primitive equations give very good results. Further tests of the performance of this scheme in the presence of physical processes will have to be conducted before we can draw a final conclusion. These experiments will have to be considered in the near future.

Compared to the explicit leapfrog scheme, each time step presently requires about 50 percent more computations; and with more efficient iterative procedures, it may be possible to reduce this figure to 20 percent. The inclusion of physical processes will also reduce this figure because these effects add computations only in the explicit part of the time step.

With a time interval six times larger in the semi-implicit model, the economy realized amounts roughly to a factor of four. This feature should appeal to most modelers. The fully implicit algorithms developed in the U.S.S.R. might provide us with an additional advantage, especially when we start using fine-mesh weather forecast models. Further experimentation with implicit methods should yield a considerable amount of information about the possibility of using these algorithms in weather forecast models or general circulation models.

REFERENCES

Holton, James R., "A Stable Finite Difference Scheme for the Linearized Vorticity and Divergence Equation System," *Journal of Applied Meteorology*, Vol. 6, No. 3, June **1967**, pp. 519–522.

Kasahara, Akira, and Washington, Warren M., "NCAR Global General Circulation Model of the Atmosphere," *Monthly Weather Review*, Vol. 95, No. 7, July **1967**, pp. 389–402.

Kurihara, Yoshio, "On the Use of Implicit and Iterative Methods for the Time Integration of the Wave Equation," *Monthly Weather Review*, Vol. 93, No. 1, Jan. **1965**, pp. 33–46.

Kwizak, Michael, and Robert, André J., "A Semi-Implicit Scheme for Grid Point Atmospheric Models of the Primitive Equations," *Monthly Weather Review*, Vol. 99, No. 1, Jan. **1971**, pp. 32–36.

Lilly, Douglas K., "On the Computational Stability of Numerical Solutions of Time-Dependent Non-Linear Geophysical Fluid Dynamics Problems," *Monthly Weather Review*, Vol. 93, No. 1, Jan. **1965**, pp. 11–26.

Marchuk, G. I., "A New Approach to the Numerical Solution of Differential Equations of Atmospheric Processes," *World Meteorological Organization Technical Note* No. 66, Geneva, Switzerland, **1965**, pp. 286–294.

McPherson, Ronald D., "Note on the Semi-Implicit Integration of a Fine Mesh Limited-Area Prediction Model on an Offset Grid," *Monthly Weather Review*, Vol. 99, No. 3, Mar. **1971**, pp. 242–246.

Mintz, Yale, "Very Long-Term Global Integration of the Primitive Equations of Atmospheric Motion," *World Meteorological Organization Technical Note* No. 66, Geneva, Switzerland, **1965**, pp. 141–167.

Robert, André J., "The Integration of a Spectral Model of the Atmosphere by the Implicit Method," *Proceedings of the WMO/IUGG Symposium on Numerical Weather Prediction, Tokyo, Japan, November 26–December 4, 1968*, Japan Meteorological Agency, Tokyo, Mar. **1969**, pp. VII–19—VII–24.

Shuman, Frederick G., and Hovermale, John B., "An Operational Six-Layer Primitive Equation Model," *Journal of Applied Meteorology*, Vol. 7, No. 4, Aug. **1968**. pp. 525–547.

Shuman, Frederick G., and Stackpole, John D., "The Currently Operational NMC Model, and Results of a Recent Simple Numerical Experiment," *Proceedings of the WMO/IUGG Symposium on Numerical Weather Prediction, Tokyo, Japan, November 26–December 4, 1968*, Japan Meteorological Agency, Tokyo, Mar. **1969**, pp. II–85—II–98.

Smagorinsky, Joseph, Manabe, Syukuro, and Holloway, J. Leith, Jr., "Numerical Results From a Nine-Level General Circulation Model of the Atmosphere," *Monthly Weather Review*, Vol. 95, No. 12, Dec. **1965**, pp. 727–768.

Thompson, Philip Duncan, *Numerical Weather Analysis and Prediction*, The Macmillan Publishing Co., New York, N.Y., **1961** 170 pp.

Young, John A., "Comparative Properties of Some Time Differencing Schemes for Linear and Nonlinear Oscillations," *Monthly Weather Review*, Vol. 96, No. 6, June **1968**, pp. 357–364

[*Received June 14, 1971; revised September 2, 1971*]